FORM TI-12
12/97

B-T-3261

STATISTICAL MODELS OF MEAN STRESS AND WATER ENVIRONMENT EFFECTS ON THE FATIGUE BEHAVIOR OF 304 STAINLESS STEEL

T. R. Leax

DE-AC11-98PN38206

NOTICE

BETTIS ATOMIC POWER LABORATORY WEST MIFFLIN, PENNSYLVANIA 15122-0079

Operated for the U.S. Department of Energy
by Bechtel Bettis, Inc.

DISCLAIMER

Portions of this document may be illegible in electronic image products. Images are produced from the best available original document.

STATISTICAL MODELS OF MEAN STRESS AND WATER ENVIRONMENT EFFECTS ON THE FATIGUE BEHAVIOR OF 304 STAINLESS STEEL

Thomas R. Leax
Bettis Atomic Power Laboratory
Bechtel Bettis, Inc.
West Mifflin, PA 15122

ABSTRACT

Recent research efforts have focused on characterizing the effects of light water reactor environments on the fatigue behavior of austenitic stainless steels. In conjunction with these experimental programs, there has been a significant effort at Argonne National Laboratory to develop statistical models for predicting the fatigue behavior of austenitic stainless steels in air and water environments at prototypical temperatures and loading rates. Some recent testing has also been concerned with the effect of mean stress on the fatigue behavior of 304 stainless steel in air. The ultimate goal of all these efforts is to allow development of fatigue design curves and design procedures that will assure adequate margin to fatigue crack initiation under prototypical operating conditions. In this paper, a best-fit strain-life curve for 304 stainless steel in air that takes into account the effect of mean stress is developed using the Smith-Watson-Topper equivalent strain parameter. A model for predicting the effect of water environments on fatigue life in both low and high oxygen water environments for a range of temperatures and loading rates is also described. Additional effort is required to develop the most appropriate way to develop a fatigue design curve from the mean stress and water effects models.

NOMENCLATURE

E = elastic modulus (MPa)
N_f = cycles to failure
R = gas constant (8.314 J/mol-K)
ε_a = strain amplitude (mm/mm)
$\dot{\varepsilon}$ = strain rate (s^{-1})
σ_a = stress amplitude at half-life (MPa)
σ_m = mean stress at half-life (MPa)
σ_{max} = maximum tensile stress at half-life (MPa)

INTRODUCTION

Neither the current ASME nor the EAC-adjusted curves proposed in NUREG/CR-5999 for 304 stainless steel apply a mean stress correction in the life regime below 10^6 cycles. The reason they do not is that the fatigue strength is higher than both the monotonic and cyclic yield strength for fatigue lives less than 10^6 cycles. Under these circumstances, most mean stress models predict that inducing a mean stress in strain or deflection control is impossible and so a mean stress correction to the design curve in this life regime is unnecessary. Unfortunately, there is little data in the literature to support or refute this hypothesis for fatigue lives less than 10^6 cycles. The ASME fatigue design curve also has no allowance for the possible detrimental effects of exposure to light water reactor (LWR) environments. While the existing ASME fatigue design factors (nominally 2X on stress and 20X on cycles) have usually been considered sufficient to cover environmental effects on austenitic stainless steel fatigue performance, recently obtained test data indicate these design factors may not be adequate for some environmental and loading conditions.

Over the last several years, there has been a substantial research effort directed at characterizing the fatigue behavior of austenitic stainless steels in LWR environments. The ultimate goal of this effort is to develop fatigue design curves and design procedures that can accurately predict the fatigue lives of reactor components in these environments. Tests have been performed on various grades of wrought, cast, and welded austenitic stainless steels in both high oxygen boiling water reactor (BWR) and low oxygen pressurized water reactor (PWR) environments over a range of temperatures and strain rates. Most of this testing has been performed by Mitsubishi Heavy Industries and Ishikawajima-Harima Heavy Industries in cooperation with a consortium of Japanese utilities, although some testing has been performed in the U.S. at Argonne

National Laboratory (ANL). In conjunction with these test programs, there has also been a significant effort to develop statistical models for predicting the fatigue behavior of austenitic stainless steels, and other reactor materials, in air and water environments at prototypical temperatures and loading rates. Much of this model development has been performed at ANL. In this paper, a best-fit fatigue curve for 304 stainless steel that conservatively accounts for the effects of mean stress is developed and a model for predicting the effect of water environments on fatigue life is described. The mean stress corrected best-fit air curve and the water effects model can be used as the basis for the subsequent development of a revised fatigue design curve and fatigue design procedure for austenitic stainless steels in LWR applications.

DATABASE

The results of strain-controlled tests on 304 stainless steel in an air environment and on 304 and 316 stainless steel in water environments are provided by Boller and Seeger (1987), Yoshida et al. (1977), Soo and Chow (1981), Jones (1983), Bernstein and Loeby (1988), Baumel and Seeger (1990), Chopra and Gavenda (1997), Conway and Stentz (1988), Rao et al. (1993), Itoh et al. (1995), Conway et al. (1975), Higuchi and Iida (1997), Kanasaki (1996), Fujiwara et al. (1986), and by the JNUFAD database. Some recent testing, reported by Wire et al. (1999), has also been conducted to quantify the effect of mean stress. In this latter program, both strain and load control tests were performed to determine whether mean stresses significantly degrade the fatigue strength.

CYCLIC STRESS-STRAIN CURVE

All of the fatigue data used in developing the cyclic stress-strain curve, with the exception of some mean strain tests reported by Wire et al. (1999), were obtained from fully reversed axial strain-control tests. The reported mean stresses in the fully reversed tests at half-life were small and, for those cases where the mean stresses were not reported, they were assumed to be zero. Wire et al. (1999) performed some axial strain controlled tests using a 1% mean strain. The sole purpose of applying a mean strain was to develop a large positive mean stress. However, the mean stresses in these tests typically relaxed with continued cycling, particularly in those specimens tested at the highest strain amplitudes. Consequently, some of Wire's tests, both with and without applied mean strains, were conducted on test specimens given twenty cycles at ± 1% strain prior to the start of testing in an effort to work harden the material and so allow, in the mean strain tests, a higher mean stress to be sustained to half-life.

Cyclic stress-strain curves were developed from the available air data (305 data points at temperatures ranging from 22°C to 427°C) by fitting the data to the following equation using the method of least squares:

$$\sigma_a = A + B \cdot \varepsilon_a \qquad (1)$$

Where: $A = A_0 + A_1 \cdot T + A_2 \cdot T^2 + A_3 \cdot precycle$

$B = B_0 + B_1 \cdot T^2 + B_2 \cdot \sigma_m + B_3 \cdot precycle$

T is the temperature (°C)

precycle is a dummy variable equal to zero if the test specimen was not precycled ± 1% prior to testing and equal to one if the test specimen was precycled ± 1% prior to testing

A_0, A_1, A_2, A_3, B_0, B_1, B_2, and B_3 are fitting constants

The fitted values for the constants from this regression analysis are as follows:

$A_0 = 175$
$A_1 = -0.342$
$A_2 = 7.10 \times 10^{-4}$
$A_3 = 53.0$
$B_0 = 24010$
$B_1 = -4.54 \times 10^{-2}$
$B_2 = 156$
$B_3 = -16080$

This cyclic stress-strain curve is valid for stresses above the proportional limit. Below the proportional limit, the stress amplitude is simply the modulus times the strain amplitude.

Figs. 1–3 provide plots comparing the predicted stress-strain curves (for no precycling and zero mean stress) at several test temperatures with the experimental data. As shown in these plots, there is good agreement between the data and the predicted stress-strain curves.

Results from Wire et al. (1999) at room temperature and 288°C are shown in Figs. 4 and 5, respectively. As reflected in Eq. (1) and as shown in these plots, specimens given a precycling treatment or subjected to an imposed mean strain tend to display higher stress amplitudes than those specimens not tested under these conditions. Positive mean stresses do not appear to affect the proportional limit, but they do significantly increase the work hardening rate. In contrast, precycling significantly increases the proportional limit while decreasing the work hardening rate. Fig. 6 provides a plot of the measured mean stress at half-life versus the measured stress amplitude normalized by the pseudo-stress amplitude ($\sigma_a/E\varepsilon_a$) for Wire's mean strain tests. The purpose of this plot is to show that large mean stresses can be sustained to half-life in strain controlled tests of 304 stainless steel when the plastic strain is a small fraction (< 20%) of the total strain. It should be noted, however, that the largest mean stresses were generated in tests where the mean strain was very high (~10%).

STRAIN-LIFE CURVE

The available air environment strain-life failure data are plotted in Fig. 7. A statistical analysis indicates that the strain-life curve is not affected by test temperature over the range of test temperatures (22°C to 427°C) represented in the database.

The method typically employed for accounting for mean stress effects relies on quantifying the effect that mean stress

has on the stress-life curve. As discussed in more detail by Wire et al. (1999), this method cannot be used to quantify mean stress effects in 304 stainless steel since an increase in mean stress correlates to an apparent increase in the fatigue strength. Consequently, mean stress effects were modeled by fitting the strain-life data to a modified version of the Smith-Watson-Topper (SWT) equivalent strain parameter (Smith et al., 1970):

$$LOG(N_f) = A + B \cdot LOG(\varepsilon_{eq} - \varepsilon_0) \qquad (2)$$

Where: ε_{eq} is the SWT equivalent strain parameter (mm/mm) given by:

$$\varepsilon_{eq} = \varepsilon_a^c \cdot (\frac{\sigma_{max}}{E})^{1-c}$$

A, B, c and ε_0 are fitting parameters

A least squares fit to the experimental data (275 data points) gave the following values for the fitted parameters:

A = -2.30
B = -2.39
c = 0.774
$\varepsilon_0 = 8.72 \times 10^{-4}$

A zero mean stress, strain-life curve can be derived from Eq. (2) by substituting into Eq. (2) a value of zero for the mean stress, a value for the strain amplitude at which a life estimate is desired, and the stress amplitude corresponding to this strain amplitude (obtained from the cyclic stress-strain curve). In deriving the strain-life curve (Fig. 8), the cyclic stress-strain curve at 288°C was used since this is near the operating temperature. However, the strain-life curve is relatively insensitive to the stress-strain curve used in its derivation since the stress term in Eq. (2) is normalized by the temperature dependent elastic modulus. The strain-life curve estimated by this procedure can be approximated by:

$$LOG(N_f) = -1.60 - 2.25 \cdot LOG(\varepsilon_a - 8.83x10^{-4}) \qquad (3)$$

This strain-life curve is compared to other proposed best-fit 304 stainless steel strain-life curves in Fig. 9. These curves include one proposed by Chopra and Smith (1998), one proposed by Jaske and O'Donnell (1977), one based on the Japanese JNUFAD database, and one used to derive the current ASME design curve. As shown in Fig. 9, the curve derived from Eq. (2) lower bounds most of the other proposed curves, particularly in the high cycle regime. The primary reason why the curve derived from Eq. (2) is more conservative than the other best-fit curves in the high cycle regime is that the fatigue life was taken as the dependent variable when performing the least squares fit. All but the Chopra and Smith fit assumed the strain amplitude was the dependent variable. Chopra and Smith use a hybrid technique, minimizing the sum of the squared Cartesian distances from the data point to the fitted curve. Assuming the strain amplitude is the dependent variable provides nonconservative estimates of the mean fatigue life in the high cycle regime. The degree of nonconservatism is a function of the amount of data scatter. However, for fatigue curves derived by assuming the fatigue life is the independent variable, the use of a factor of two on stress (strain) to obtain the design curve may more than compensate for the nonconservative curve fit.

Using the SWT formulation makes it is easy to correct the best fit zero mean stress strain-life curve for the maximum effect of mean stress. In the present case, this was accomplished simply by assuming that the maximum stress in Eq. (2) can never fall below 337 MPa (the estimated stress amplitude at 288°C when the strain amplitude is one percent); a relatively conservative assumption. The resulting strain-life curve is shown in Fig. 8. At 10^6 cycles, the strain-life curve corrected for the maximum effect of mean stress is lower than the best fit curve by a factor of approximately 1.25. For the assumed maximum stress of 337 MPa ksi, this represents a mean stress of 175 MPa at 10^6 cycles, which is slightly higher than the highest mean stress observed at half-life in the Wire et al. (1999) mean strain tests (Fig. 6).

EFFECT OF A WATER ENVIRONMENT

Fatigue data obtained on austenitic stainless steels in water environments are plotted in Fig. 10. While sensitization can have a profound and detrimental effect of the fatigue life of austenitic stainless steels in high oxygen BWR water (there is no effect in low oxygen PWR water), test results on sensitized materials tested in BWR water are not included in the present analysis. This aspect of the fatigue behavior of 304 stainless steel is beyond the scope of this paper.

The apparently large data scatter evident in Fig. 10 is due, in large part, to the effects of testing at different temperatures and strain rates. Unlike the behavior in air, test temperature and loading rate can have a profound effect on the fatigue behavior in water. Test results on three types of austenitic stainless steel (304, 316, and 316NG) at temperatures ranging from 100°C to 360°C and at strain rates ranging from 10^{-6} s^{-1} to 10^{-1} s^{-1} are included in the database. In addition, a few test results on 316NG welds are also included in the database. Tests were run in both BWR primary water (dissolved oxygen [DO] of 200 ppb or higher) and PWR primary water (dissolved oxygen less than 20 ppb). The majority of testing was in strain control, but a few long life tests were performed in load control. Strains in the load control tests were estimated from the cyclic stress-strain curve.

The statistical model developed for predicting the effect of water environments on the fatigue life has the following form:

$$N_f = A \cdot (\varepsilon_a - \varepsilon_0)^b \cdot \left[P + (1-P) \cdot e^{-kt_{eff}^m} \right] \qquad (4)$$

Where: A, b, ε_0, P, k, and m are fitting constants
t_{eff} is a time-temperature parameter with units of seconds and is given by:

$$t_{eff} = \frac{\varepsilon_a}{\dot{\varepsilon}} e^{\frac{-Q}{RT}}$$

T is the temperature (K)
Q is the fitted value of the activation energy (kJ/mol)

The first part of the expression on the right hand side of Eq. (4) (i.e., $A(\varepsilon_a - \varepsilon_0)^b$) represents the expected fatigue life, in water, at low temperatures and high strain rates. P is a measure of the maximum expected degradation at low strain rates and high temperatures. A value for P of one indicates that strain rate and temperature have no effect on the fatigue behavior in water, while a value for P of zero indicates that the fatigue life goes to zero at sufficiently high temperatures and low strain rates. When P is between zero and one, the effect of water saturates at sufficiently high temperatures and/or low strain rates.

For convenience in comparing the air and water fatigue curves, the value of b was taken to be the same as the slope of the strain-life curve in air (i.e., -2.25) and the value for ε_0 was taken to be the same as for the air curve (i.e., 8.83×10^{-4}). Determining the values of these parameters from the regression analysis, rather than assuming the air values, has only a small effect on the goodness of fit (an increase in the correlation coefficient, r^2, from 0.952 to 0.954), thus justifying this approach. Further, most of this increase in r^2 is due to a better fit of two long life data points both tested at a strain amplitude of 1.2×10^{-3} mm/mm.

A least squares fit of the data (246 points) to the logarithm of both sides of Eq. (4), with the assumption that the values of b and ε_0 are the same as for the air curve, results in the following values for the remaining constants:

$$LOG(A) = -1.88 + 0.181 \bullet Material + 0.274 \bullet Oxygen$$
$$P = 0.152$$
$$k = 0.215 \cdot \varepsilon_a^{-1.15} \text{ for low oxygen water (DO < 20 ppb)}$$
$$k = 1.21x10^6 \cdot \varepsilon_a^{-1.15} \text{ for high oxygen water (DO} \geq \text{200 ppb)}$$
$$Q = 69.6 \text{ kJ / mol for low oxygen water}$$
$$Q = 248 \text{ kJ / mol for high oxygen water}$$
$$m = 0.397$$

Where: Material = 0 for 304 SS or 316 SS and Material = 1 for 316NG SS
Oxygen = 0 when DO < 20 ppb and Oxygen = 1 when DO ≥ 200 ppb

There was no statistically significant difference between the behavior of 304 stainless steel and 316 stainless steel, nor was there a difference in the behavior of wrought versus welded 316NG. The fatigue properties of 316NG stainless steel do, however, appear to be superior to those of both 304 and 316 stainless steel. Also, there was no significant effect of the mode of loading (strain versus load control). Load control was only used for high cycle fatigue tests where the use of strain control was not feasible. Consequently, the strains, which were estimated from the cyclic stress-strain curve, were predominantly elastic.

A comparison of the observed versus fitted values of cycles to failure using the model described above is shown in Fig. 11. The model provides a very good description of the test data over the range of the available data.

As noted above, the fatigue life in water at low temperatures and high strain rates is given by $N_f = A \cdot (\varepsilon_a - \varepsilon_0)^b$. A comparison of the 304 stainless steel air curve with the low and high oxygen water curves under low temperature and high strain rate conditions indicates that the air and high oxygen water curve are virtually identical, while the low oxygen water curve is lower than the air curve by a factor of 1.9 on life.

The observed fatigue life for each test condition was normalized by dividing by the predicted fatigue life under low temperature, high strain rate conditions (i.e., by $N_f = A \cdot (\varepsilon_a - \varepsilon_0)^b$). A plot of the normalized fatigue life versus the time-temperature parameter ($kt_{eff}^{\ m}$) is shown in Fig. 12. This plot provides justification for the concept that the effect of water saturates at sufficiently high temperatures and low strain rates in both high and low oxygen water environments.

The model developed above was used to predict the fatigue life of 304 stainless steel at various temperatures, strain rates, and strain amplitudes. The results of these predictions are shown in Figs. 13 and 14 for low oxygen water environments and in Figs. 15 and 16 for high oxygen water environments. In these figures, the reciprocal of the normalized fatigue life (defined above) multiplied by the difference between the air curve and the low temperature, high strain rate water curve (i.e., a factor of one for high oxygen water and a factor of 1.9 for low oxygen water) is defined as the water reduction factor. This is the factor on life needed to bring the best-fit air and water curves into coincidence for a given temperature, strain rate, and strain amplitude. The model predicts that the water reduction factor can be as much as a factor of 12.5 on life in a low oxygen water environment and as much as a factor of 6.6 on life in a high oxygen water environment when the temperature is high and the strain rate is low. Plots comparing the model predictions with selected subsets of the data for a low oxygen water environment are shown in Figs. 17-20.

When making predictions from models derived from data sets where there are a large number of independent variables, it is important to identify the range over which the independent variables were varied. Otherwise, it is difficult to determine whether a given model prediction is within the range of the data or whether it is an extrapolation well beyond the range of the data. Model predictions outside the range of the data could potentially lead to nonconservative, or overly conservative, life predictions. The approximate range of the test conditions where data are available is noted in Figs. 13-16.

The estimated activation energies for low and high oxygen water are significantly different (69.6 kJ/mol and 248 kJ/mol, respectively). As a consequence, a small change in temperature has a larger effect on the water reduction factor for high oxygen water than for low oxygen water as is evident when comparing the plots in Figs. 14 (low oxygen water) and 16 (high oxygen water). Since many of the predictions shown in these figures are at conditions well beyond any in the database, caution is required when applying these predictions to actual service conditions. In particular, the activation energy for high oxygen water was estimated from tests over a relatively narrow temperature range (288°C to 325°C) and so may not provide an accurate estimate of the fatigue behavior in high oxygen water at low temperatures.

COMPARISON WITH THE ANL LWR ENVIRONMENT MODEL

ANL has been compiling fatigue data on pressure boundary materials in LWR environments with the objective of assessing the ASME Code fatigue design curves and design criteria. ANL has performed statistical analyses of these data and has developed empirical models and interim design curves describing the air and LWR environment fatigue behavior of several reactor materials. Materials evaluated include carbon and low alloy steels, stainless steels, and nickel base alloys. Recent ANL assessments of the fatigue behavior of austenitic stainless steels in air and LWR environments are given by Chopra and Gavenda (1997), Chopra and Smith (1998), Majumdar et al. (1993), and Keisler et al. (1995, 1996).

The database used by ANL for modeling the fatigue behavior of austenitic stainless steels in water includes the data in Fig. 10, but is slightly larger (290 versus 257 data points). The major difference is that the ANL database contains test results obtained by Hale et al. (1977, 1981) who tested 304 and 304L stainless steel in 260°C air and BWR water. The tests in BWR water were nominally at four cycles per hour, but since the rise time in each cycle was only 10s-20s, with a hold time at the maximum deflection, the strain rates were considerably higher than would be implied by the test frequency. These results are not included in the present database since they were obtained from cantilever beam specimens tested in deflection control. However, the test results are qualitatively consistent with the model predictions shown in Fig. 16.

ANL's latest model describing the fatigue behavior of austenitic stainless steels in water environments is given by Chopra and Smith (1998). For a given strain amplitude, the fatigue life in air based on ANL's model is a factor of 2.55 higher than the fatigue life in water at low temperatures and/or high strain rates. ANL's model (including the factor of 2.55) predicts that, at high temperatures and low strain rates, the fatigue life can be reduced by as much as a factor of 15.3 in a low oxygen water environment and by a factor of 8.3 in a high oxygen water environment compared to the fatigue life in air. This is similar to the predictions of the Eq. (4) model.

Although, the Eq. (4) model and the ANL model provide similar predictions at the test conditions represented in the database, predictions for temperatures and strain rates outside the database can be quite different. ANL's model predicts no change in the fatigue life with decreasing strain rates at temperatures below 200°C, other than the factor of 2.55, whereas the Eq. (4) model indicates there can be a substantial penalty under some loading conditions, particularly in low oxygen water. In the ANL model, the water reduction factor is only a function of strain rate and does not depend on temperature for temperatures above 200°C. In the Eq. (4) model, both the strain rate and temperature have a large effect on the water reduction factor. The Eq. (4) model also predicts that, at a given strain rate and temperature, the water reduction factor increases with decreasing strain amplitude. In contrast, the ANL model predicts no dependence on strain amplitude. Finally, the Eq. (4) model predicts a significantly different temperature dependence for high and low oxygen water while the ANL model predicts no difference.

DISCUSSION

Sufficient data now exist to allow development of a fatigue design curve for 304 stainless steel in air that accurately accounts for the effects of mean stress. However, there is no simple way to develop a single design curve applicable to water environments that is not either overly conservative or nonconservative depending on the specific environmental and loading conditions. Use of a worst case water reduction factor of approximately thirteen for low oxygen water would result in a design factor of 130 on the best-fit air curve (assuming the design factor of 20 on cycles already contains a factor of two for environment), and so would effectively preclude the use of 304 stainless steel in many components exposed to water. On the other hand, ignoring the effect of environment could result in premature cracking. Figures 13-16 show that even at high temperatures there are regimes of strain amplitude and strain rate where the effect of water is relatively minor, thus making the use of 304 stainless steel in component design a viable option for these loading conditions. One approach for incorporating water effects into the design procedure, developed by Mehta and Gosselin (1995), applies a water reduction factor to the partial usage factor calculated for each transient. The specific water reduction factor (environmental correction factor, K_{en}, in Mehta's nomenclature) used for each transient depends on the temperature and loading conditions for that transient. Since the temperature and strain rate may not be constant during a given transient, Mehta and Gosselin have developed procedures for determining the effective values of these parameters for a given transient to use in calculating the appropriate water reduction factor. Mehta and Gosselin have also proposed changes to the fatigue evaluation procedures in Section III of the ASME code that are needed to implement their proposed approach. Another approach, proposed by Chopra and Smith (1998), is to use strain-rate dependent fatigue design curves developed from ANL's statistical model. These proposed methods have not been enthusiastically embraced, primarily since their adoption would result in much more conservative fatigue life predictions for LWR environments. Given the complex issues involved in developing a design curve

applicable to LWR environments, additional work is required to develop a consensus position prior to recommending changes to the 304 stainless steel design curve. Some additional testing may also be required at temperatures and loading conditions not in the current database, but which may be encountered in service, in order to resolve differences in the Eq. (4) environmental effects model and the ANL model.

SUMMARY AND CONCLUSIONS

The available fatigue data on 304 stainless steel indicate that mean stress has a relatively modest effect on the fatigue behavior, but that water environments can cause a significant decrease in the fatigue life under some loading conditions. Based on the available fatigue data, a model has been developed using the Smith-Watson-Topper equivalent strain parameter that can be used to develop a 304 stainless steel fatigue design curve corrected for the maximum effect of mean stress. This model predicts a reduction in the fatigue strength of approximately 25% at 10^6 cycles for an applied mean stress of 175 MPa. A model has also been developed that allows fatigue life predictions for 304 stainless steel in both low and high oxygen water environments at prototypical temperatures and loading rates. This model indicates that the fatigue life of 304 stainless steel in water depends on the temperature, strain rate, applied strain amplitude, and water oxygen level. For low oxygen water, the fatigue life can be reduced by as much as factor of thirteen at high temperatures and low strain rates. For high oxygen water, the fatigue life can be reduced by as much as a factor of seven. The mean stress corrected air curve and the water effects model can be used as the basis for developing a revised fatigue design curve and fatigue design procedure for 304 stainless steel for LWR applications. Given that the conventional approach of using a worst case water reduction factor would result in a prohibitively large design factor and so effectively preclude the use of austenitic stainless steel in many components exposed to water, additional effort is required to determine the most appropriate way to incorporate the mean stress and water effects models into a design curve. Some steps in this direction have already been taken by Mehta and Gosselin (1995) and by Chopra and Smith (1998). Additional testing may also be required at prototypical temperatures and loading rates that are outside the current database in order to resolve differences in the predicted fatigue lives between the model presented here and the ANL model.

ACKNOWLEDGEMENTS

This work was performed under a U. S. Department of Energy contract with the Bettis Atomic Power Laboratory, operated by Bechtel Bettis, Inc. The author would like to thank D. G. Rapp and A. J. DiNicola for their helpful discussions in the preparation of this paper.

REFERENCES

Baumel, A., and Seeger, T., 1990, Materials Data for Cyclic Loading Supplement 1, Elsevier Science Publishers B. V., Amsterdam, The Netherlands, pp. C10-C12

Bernstein, H., and Loeby, C., 1988, "Low-Cycle Corrosion Fatigue of Three Engineering Alloys in Salt Water", J. Eng. Mat. & Tech., Vol. 110, pp. 234-239

Boller, C., and Seeger, T., 1987, Materials Data for Cyclic Loading Part C: High Alloyed Steels, Elsevier Science Publishers B. V., Amsterdam, The Netherlands, pp. 77-79

Chopra, O. K., and Gavenda, D. J., 1997. "Effects of LWR Coolant Environments on Fatigue Lives of Austenitic Stainless Steels", Pressure Vessel and Piping Codes and Standards, PVP Vol. 353, D. P. Jones, B. R. Newton, W. J. O'Donnell, R. Vecchio, G. A. Antaki, D. Bhavani, N. G. Cofie and G. L. Hollinger, eds., ASME, pp. 87-97

Chopra, O. K., and Smith, J. L., 1998, "Estimation of Fatigue Strain-Life Curves for Austenitic Stainless Steels in Light Water Reactor Environments", Fatigue, Environmental Factors, and New Materials, H. S. Mehta, ed., PVP Vol. 374, ASME, pp. 249-259

Conway, J. B., Stentz, R. H., and Berling, J. T., 1975, Fatigue, Tensile, and Relaxation Behavior of Stainless Steels, TID-26135, Mar-Test, Inc., Cincinnati, OH

Conway, J. B., and Stentz, R. H., 1988, "Fatigue Characteristics of Wrought and Cast Carbon Steel and 304 Stainless Steel", Fatigue Initiation, Propagation, and Analysis for Code Construction, M. Prager, ed., MPC Vol. 29, ASME, pp. 1-50

Fujiwara, M., Endo, T., and Kanasaki, H., 1986, "Strain Rate Effects on the Low Cycle Fatigue Strength of 304 Stainless Steel in High Temperature Water Environment", Fatigue Life: Analysis and Prediction, Proceedings of the International Conference and Exposition on Fatigue, Corrosion Cracking, Fracture Mechanics, and Failure Analysis, ASM, Metals Park, OH, pp. 309-313

Hale, D. A., Wilson, S. A., Kiss, E., and Giannuzzi, A. J., 1977, "Low Cycle Fatigue Evaluation of Primary Piping Materials in a BWR Environment", GEAP-20244, NRC-5, General Electric Corp.

Hale, D. A., Wilson, S. A., Kass, J. W., and Kiss, E., 1981, "Low Cycle Fatigue of Commercial Piping Steels in a BWR Primary Water Environment" J. Eng. Materials & Technology, Vol. 103, pp. 15-25

Higuchi, M., and Iida, K., 1997, "Reduction in Low-Cycle Fatigue Life of Austenitic Stainless Steels in High-Temperature Water", Pressure Vessel and Piping Codes and Standards, PVP Vol. 353, D. P. Jones, B. R. Newton, W. J. O'Donnell, R. Vecchio, G. A. Antaki, D. Bhavani, N. G. Cofie and G. L. Hollinger, eds., ASME, pp. 79-85

Itoh, T., Sakane, M., Ohnami, M., and Socie, D. F., 1995, "Nonproportional Low Cycle Fatigue Criterion for Type 304 Stainless Steel", J. Engrg. Mat. & Tech., Vol. 117, pp. 285-292

Jaske, C. E., and O'Donnell, W. J., 1977, "Fatigue Design Criteria for Pressure Vessel Alloys", J. Pressure Vessel Technology, Trans. ASME, Vol. 99, pp. 584-592

Jones, D. J., 1983, "Extension of Simple Cyclic Fatigue Damage Characteristics to Multiaxial Life Prediction Methods", Univ. of Illinois [see also: Jones, D. J., and Kurath, P., 1988, "Cyclic Fatigue Damage Characteristics Observed for Simple Loadings Extended to Multiaxial Life Prediction", NASA Contractor Report 182126]

Kanasaki, H., 1996, "Fatigue Life of Stainless Steels and Alloy 600 in PWR Primary Water", presented at the Pressure Vessel Research Council Meeting, October 7-9, Columbus, OH

Keisler, J., Chopra, O. K., and Shack, W. J., 1995, "Fatigue Strain-Life Behavior of Carbon and Low-Alloy Steels, Austenitic Stainless Steels, and Alloy 600 in LWR Environments", NUREG/CR-6335, ANL 95/15, Argonne National Laboratory

Keisler, J. M., Chopra, O. K., and Shack, W. J., 1996, "Statistical Models for Estimating Fatigue Strain-Life Behavior of Pressure Boundary Materials in Light Water Reactor Environments" Nuclear Engineering & Design, Vol. 167, pp. 129-154

Majumdar, S., Chopra, O. K., and Shack, W. J.,1993, "Interim Fatigue Design Curves for Carbon, Low-Alloy, and Austenitic Stainless Steels in LWR Environments", NUREG/CR-5999, ANL-93/3, Argonne National Laboratory

Mehta, H. S., and Gosselin, S. R., 1995, "An Environmental Factor Approach to Account for Reactor Water Effects in Light Water Reactor Pressure Vessel and Piping Fatigue Evaluations", EPRI TR-105759, Final Report, EPRI

Rao, K. B. S., Valsan, M., Sandhya, R., Mannan, S. L., and Rodriguez, P., 1993, "An Assessment of Cold Work Effects on Strain-Controlled Low-Cycle Fatigue Behavior of Type 304 Stainless Steel", Met. Trans. A, Vol. 24A, pp. 913-924

Smith, K. N., Watson, P., and Topper, T. H., 1970, "A Stress-Strain Function for the Fatigue of Metals", J. Materials, ASTM, Vol. 5, No. 4, pp. 767-778

Soo, P., and Chow, J. G. Y., 1981, "Development of a Procedure for Estimating the High Cycle Fatigue Strength of Some High Temperature Structural Alloys", J. Eng. Mat. & Tech., Vol. 103, pp. 97-103

Wire, G. L., Leax, T. R., and Kandra, J. T., 1999, "Mean Stress Effects on Fatigue in Type 304 Stainless Steel and Additional Data on Notch Effects", presented at the 1999 ASME PVP Conference, Boston, MA, available at OSTI, B-T-3262

Yoshida, S., Kanazawa, K.,Yamaguchi, K., Sasaki, M., Kobayashi, K., and Sato, M.,1977, "Elevated Temperature Fatigue Properties of Engineering Materials Part I", Trans. of the National Research Inst. For Metals, Tokyo, Vol. 19, No. 5, pp. 247-272

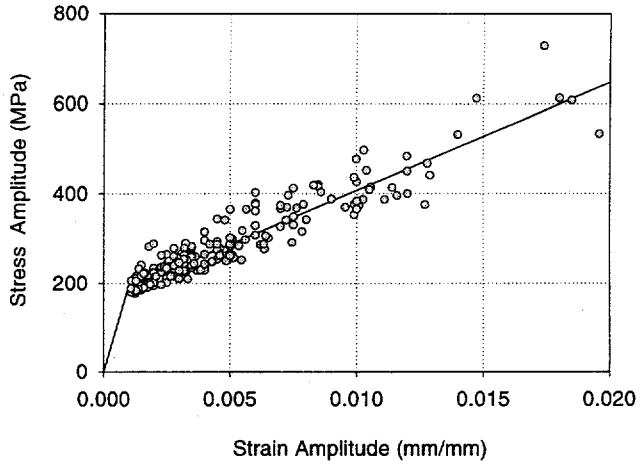

Figure 1 Room temperature cyclic stress-strain curve.

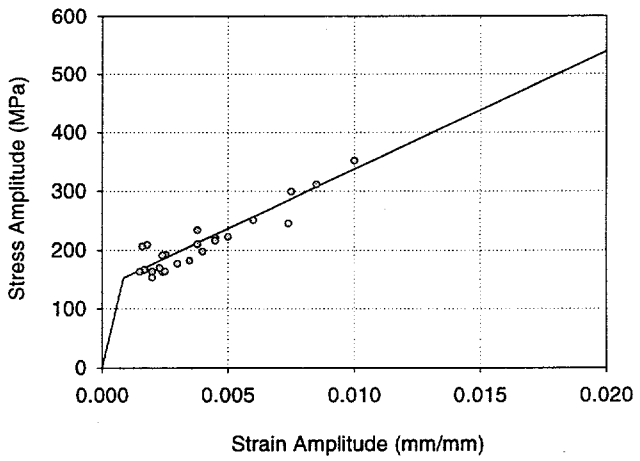

Figure 2 288°C cyclic stress-strain curve.

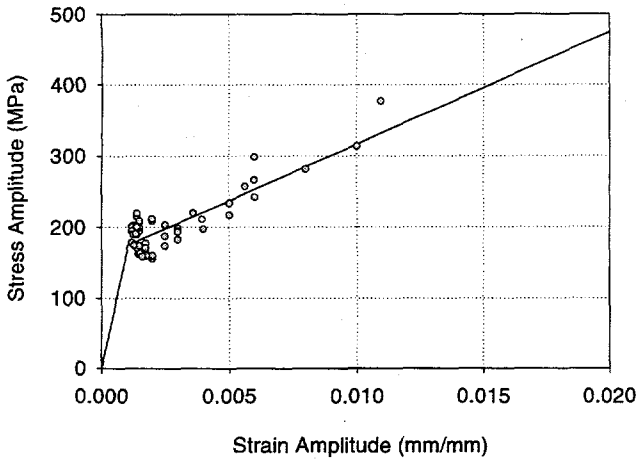

Figure 3 427°C cyclic stress-strain curve.

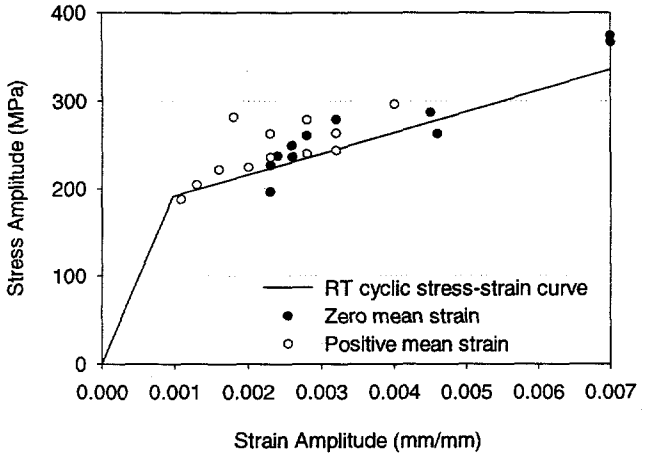

Figure 4 Room temperature cyclic stress-strain data from Wire et al. (1999).

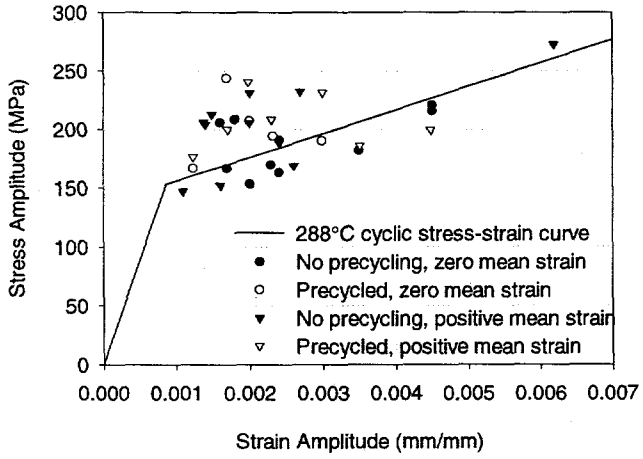

Figure 5 288°C cyclic stress-strain data from Wire et al. (1999).

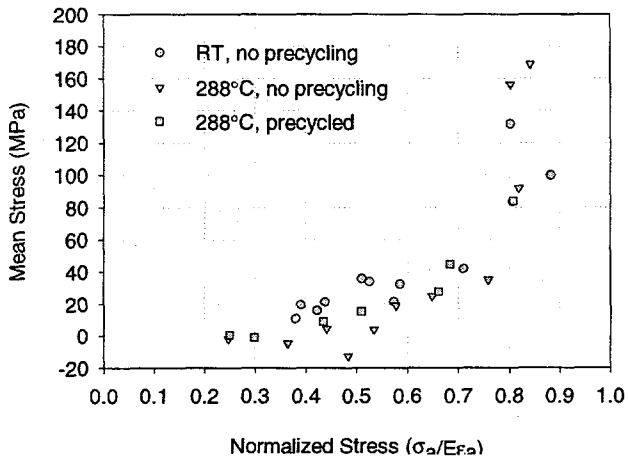

Figure 6 The measured mean stress at half-life versus the normalized stress amplitude in the Wire et al. (1999) mean strain tests. A normalized stress amplitude equal to one indicates completely elastic loading.

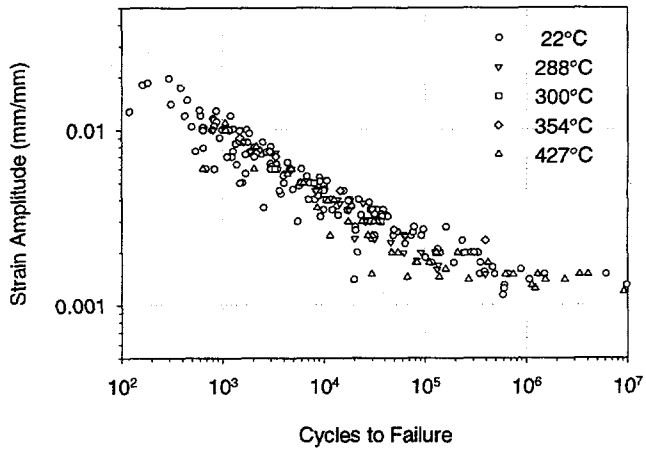

Figure 7 Air environment strain-life data for 304 stainless steel.

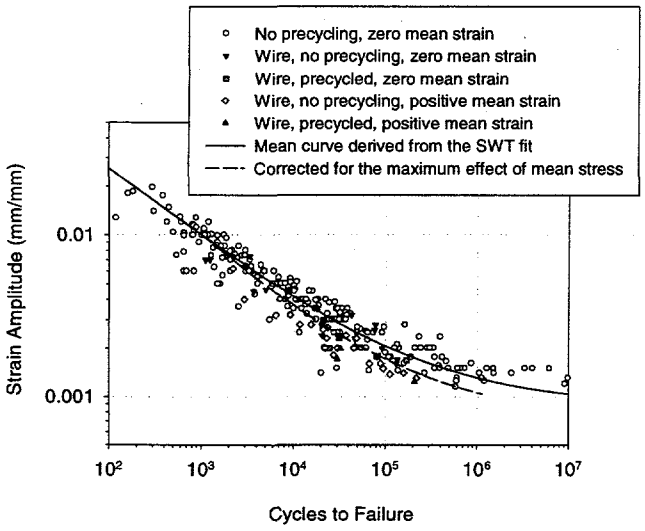

Figure 8 Best fit strain-life curve without and without a mean stress correction.

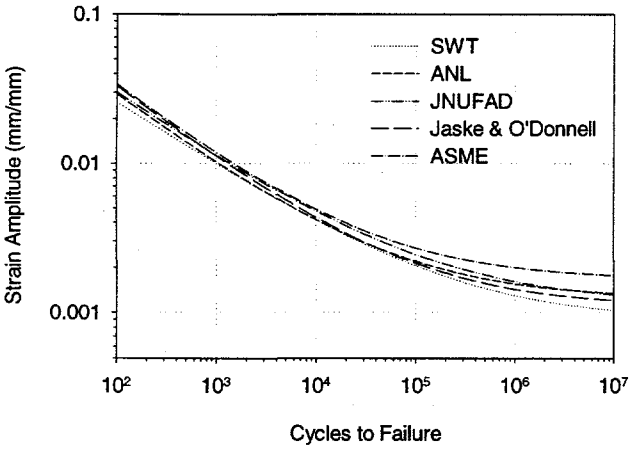

Figure 9 Comparison of several zero mean stress strain-life curves for 304 SS. References for these curves are provided in the text.

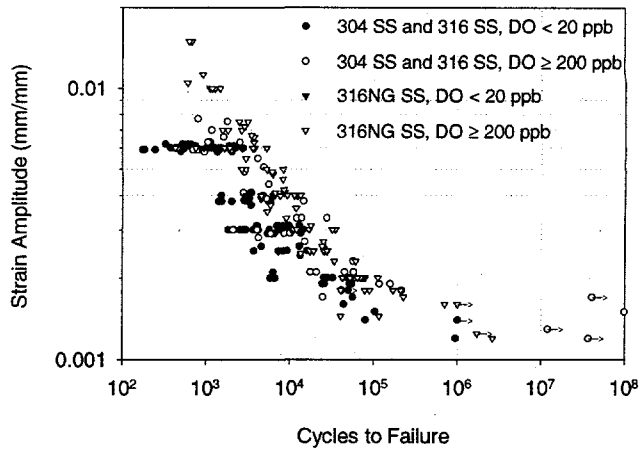

Figure 10 Strain-life data for 304 and 316 stainless steel in water.

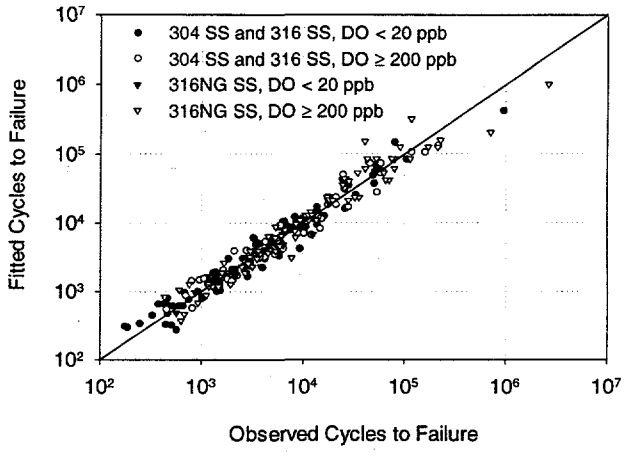

Figure 11 Observed versus fitted cycles to failure.

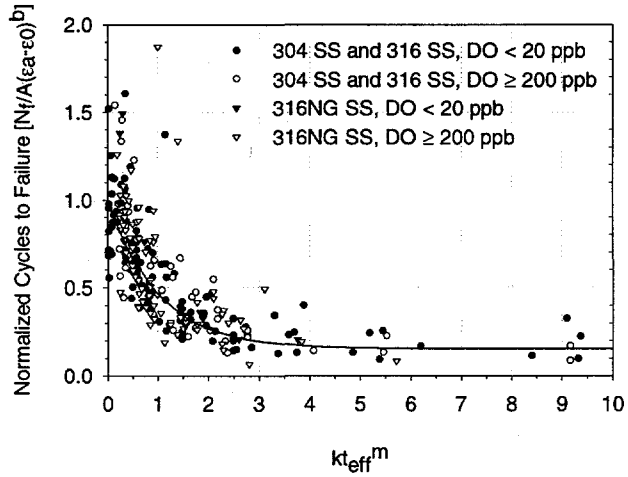

Figure 12 Normalized fatigue life as a function of the time-temperature parameter showing threshold (saturation) behavior.

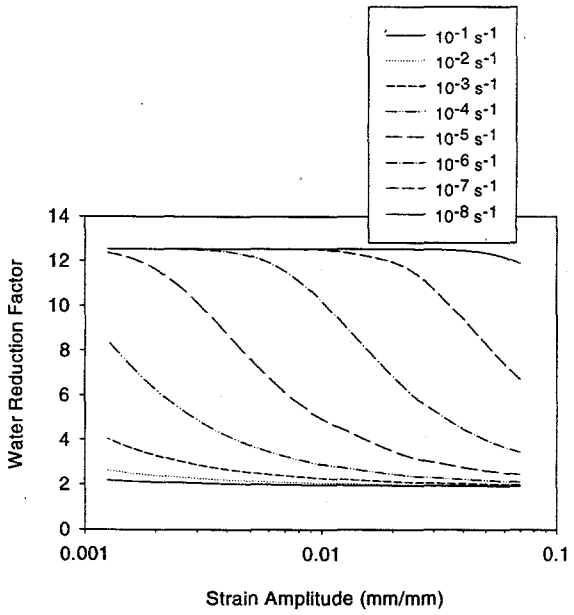

Figure 13 Predicted water reduction factors for 304 SS in low DO water at 260°C. Test data are available at strain amplitudes in the range from 0.002 mm/mm to 0.006 mm/mm and at strain rates in the range from 10^{-1} s^{-1} to 10^{-5} s^{-1} Predictions outside these ranges are extrapolations.

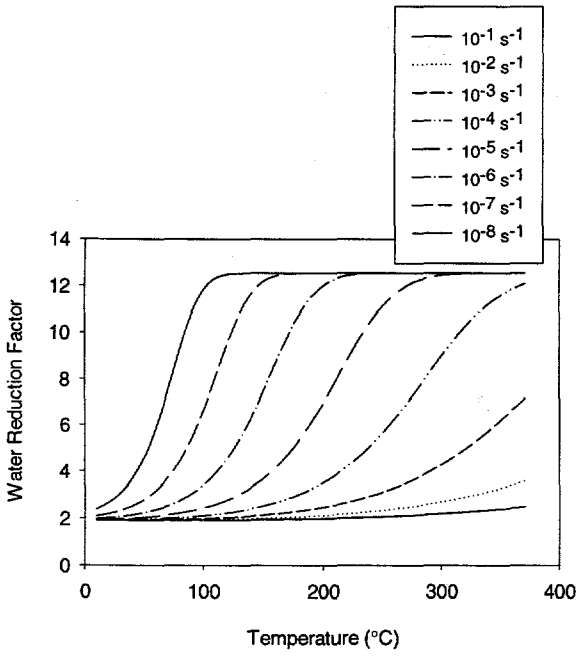

Figure 14 Predicted water reduction factors for 304 SS in low DO water as a function of temperature and strain rate. The strain amplitude was assumed to be 0.002 mm/mm. Test data are available at temperatures in the range from 100°C to 360°C and at strain rates in the range from 10^{-2} s^{-1} to 10^{-5} s^{-1}. Predictions outside these ranges are extrapolations.

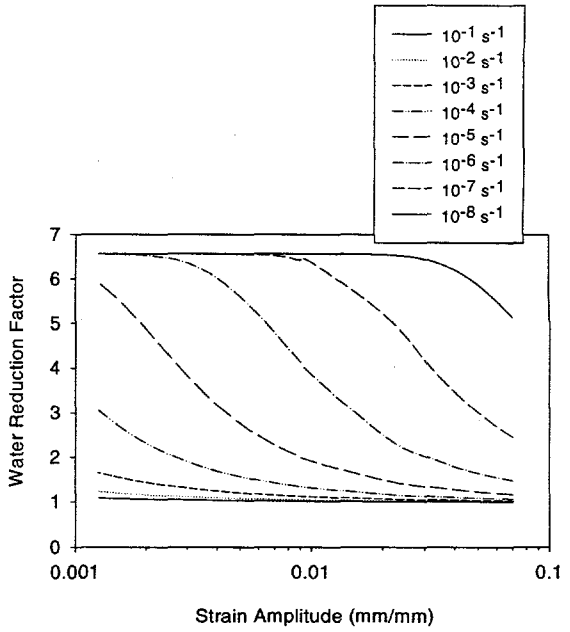

Figure 15 Predicted water reduction factors for 304 SS in high DO water at 260°C. Test data are available at strain amplitudes in the range from 0.012 mm/mm to 0.008 mm/mm and at strain rates in the range from 10^{-1} s^{-1} to 10^{-4} s^{-1}. Predictions outside these ranges are extrapolations.

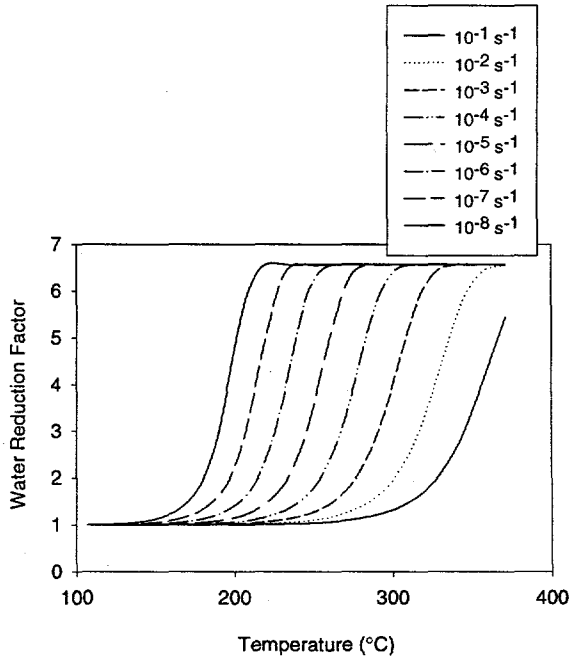

Figure 16 Predicted water reduction factors for 304 SS in high DO water as a function of temperature and strain rate. The strain amplitude was assumed to be 0.002 mm/mm. Test data are available at temperatures in the range from 288°C to 325°C and at strain rates in the range from 10^{-1} s^{-1} to 10^{-5} s^{-1}. Predictions outside these ranges are extrapolations.

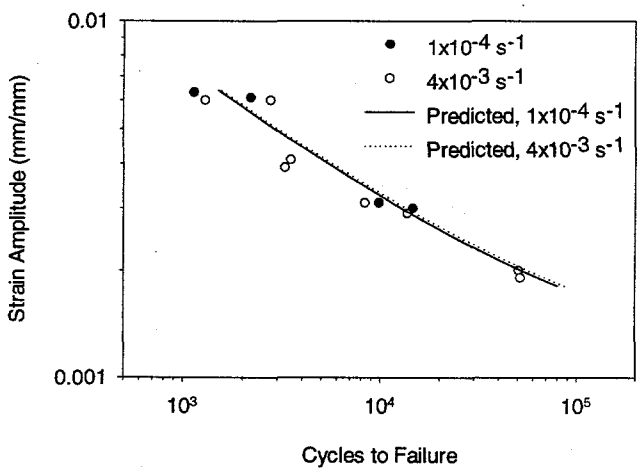

Figure 17 Strain-life behavior of 304 and 316 stainless steel at 100°C in low oxygen water.

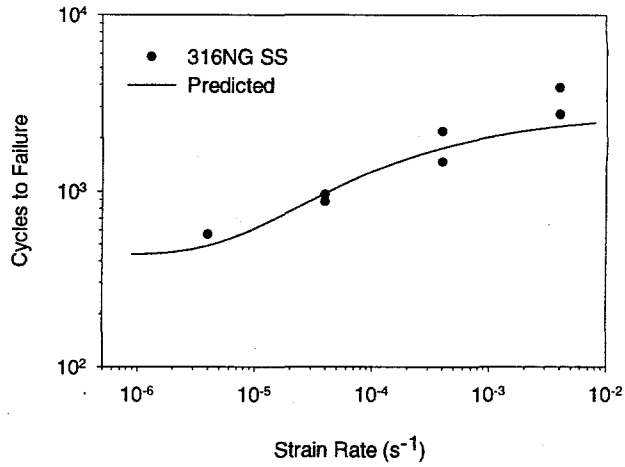

Figure 19 Effect of strain rate on the fatigue life of 316NG stainless steel at 290°C in low oxygen water at a strain amplitude of 0.006 mm/mm.

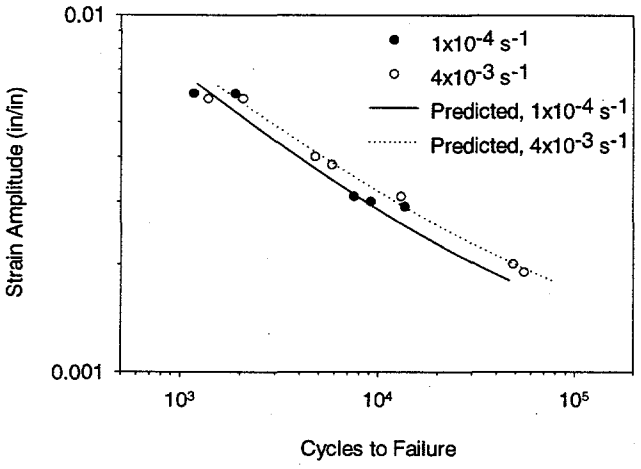

Figure 18 Strain-life behavior of 304 and 316 stainless steel at 200°C in low oxygen water.

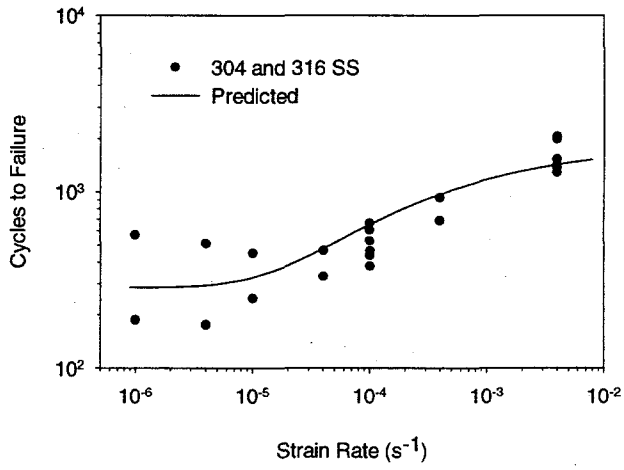

Figure 20 Effect of strain rate on the fatigue life of 304 and 316 stainless steel at 325°C at a strain amplitude of 0.006 mm/mm.